Temperature Profiles in Home Ovens and Refrigerators

Nayan Myerson-Jain, John Wang, Zhaoqi Wu, Steven Zhang
University of Illinois at Urbana-Champaign
PHYS 398 DLP

Spring 2020

Abstract

In this report, we analyze mean temperature fields in home appliances such as ovens and refrigerators. For a holistic approach, we utilize multiple thermocouples soldered to a printed circuit board to record temperature data at multiple different points inside these appliances for different runs of data taking. The goal of this project is an exploratory one; our purpose is to learn more about the appliances as well as the instruments used in our experiments by examining the temperature fields inside ovens and refrigerators. The number of thermocouples available to be soldered onto a single circuit board as well as the fragility of the experimental equipment plays a large role in the uncertainty in our data and calculations, but the behavior of temperature profiles inside these appliances is clear.

Introduction

Ovens and refrigerators are instruments that are everyday appliances and are readily available to almost everyone, but people rarely investigate their distinguishing features. For instance, some of these features may be temperature profiles, thermal diffusivity, and power efficiency which can have a non-negligible influence on their usage. Different cooking and baking techniques may require different levels of precision of an oven - incorrect temperature profiles and humidity may result in poor results from baking and cooking inside the oven being used. Different types of ovens work in different ways and are equipped with a wide range of components. Therefore both the temperature fields and gradients inside them may be drastically different. Even in the same oven, temperature profiles are not uniform in space and can differ by quite a lot depending on the make and condition.

In our project, we use thermocouples to measure the temperatures at a discrete set of positions inside a plane of fixed elevation in the oven. The thermocouples are soldered onto a printed circuit board, which supports an Arduino and other devices allowing us to read and store the data taken. The data is stored in an SD card, which is later used to produce plots of the temperature of each thermocouple versus time for these different positions. The gradient of the temperature is then reconstructed by other means of modeling. In this fashion, we hope to understand the various features of an oven. For instance, the temperature profile, heat insulation, the error between set and actual temperature.

Finally, we wish to compare our results to the temperature profiles of theoretical models. In particular, we look to see if the temperature profile data taken by our thermocouples matches well with smooth solutions to the heat equation. While they will not match exactly, we look for similar behavior and what possible sources of error make come about from the conditions of the experiment and oven.

1 Background

1.1 Instrumentation

1.1.1 Arduino Mega 2560

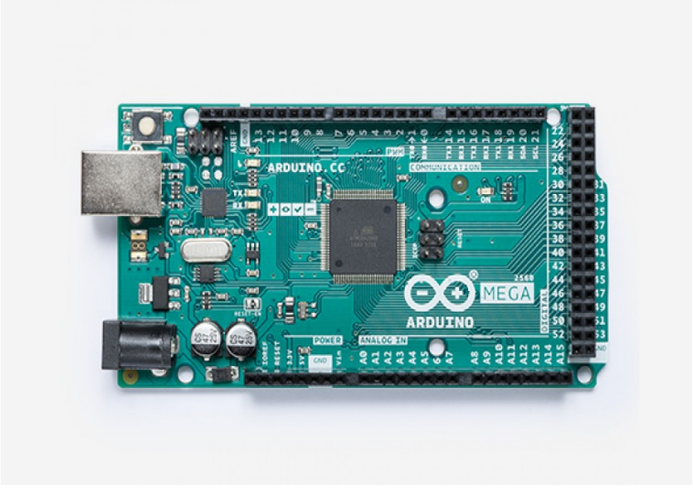

Figure 1: Arduino Mega 2560

For our project, we used the Arduino Mega 2560 microcontroller, shown in Figure 1, as the primary device to link the Data-Acquisition together. The Arduino Mega 2560 is a microcontroller board that has 54 digital input/output pins, 16 analog inputs, 4 hardware serial ports, a clock speed of 16 MHz and two communication protocols which are Serial Peripheral Interface (SPI) and Inter-Integrated Circuit communication (I2C). We mainly use the SPI protocol to communicate with other breakout board sensors. All the chips are soldered on the printed circuit board.

1.1.2 Thermocouple Amplifier

The K type thermocouples (Figure 2) are very sensitive temperature sensors and made by welding together two metal wires. Because of the physical effect of two joined metals, there is a slight voltage across the wires that increases with temperature. Base on the voltage difference, it can measure the temperature range from $-200°C$ to $1350°C$ in $0.25°C$ increments and have about $\pm 2°C$ to $\pm 6°C$ accuracy. This amplifier breakout board has the chip itself, a $3.3V$ regulator with 10 bypass capacitors and level shifting circuitry and uses SPI data output which requires any 3 digital I/O pins from the Arduino Mega 2560.

1.1.3 BME680

The BME680 (Figure 3) is a 4-in-1 sensor with humidity, gas, atmospheric pressure and temperature measurement based on proven sensing principles. Main measurement characteristics: humidity accuracy ± 3 percent with response time $(0 - 0.63)$, resolution of gas sensor

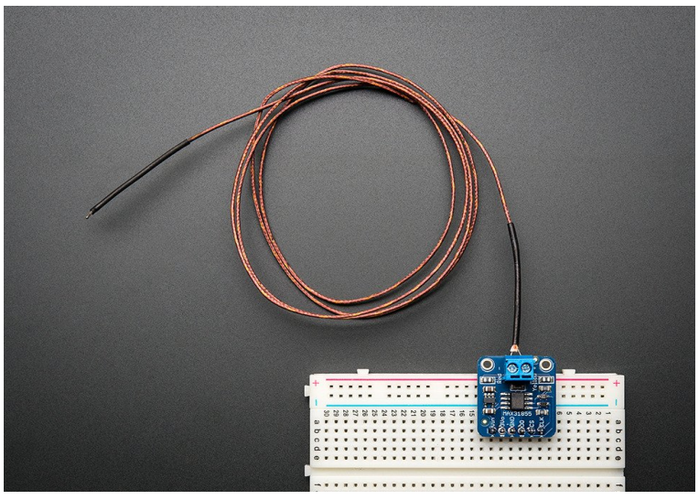

Figure 2: Adafruit MAX31855 Thermocouple and Amplifier Breakout Board

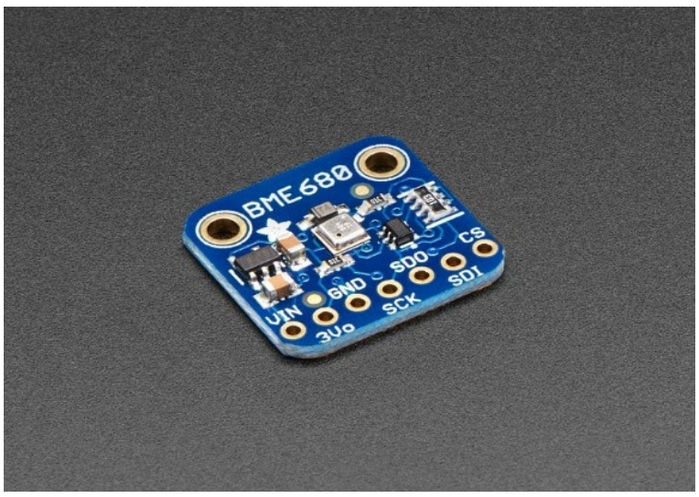

Figure 3: Adafruit BME680

resistance measurement 0.05-0.11 percent with response time $(0.33-0.63)$, absolute temperature $(0-65°C)$ accuracy $\pm 1°C$ and absolute/relative pressure accuracy $\pm 0.6hPa/\pm 0.12hPa$ (EDN Europe, 2015).BME680 equips with both SPI and I2C interfaces to connect it to the Arduino using only 4 wires which are the serial clock (SCK), the serial data input (SDI), the serial data output (SDO) and the chip select (CS). We mainly use BME680 to collect the humidity inside the refrigerator while the thermocouples are collecting the temperature data.

1.1.4 Printed Circuit Board

The printed circuit board is designed and provided by the course instructor Professor Gollin. The challenge of making the PCB is to figure out how to arrange the thermocouple amplifiers. The thermocouple amplifier uses SPI communication protocol which is a synchronous serial communication interface primarily used in embedded systems (e.g. Arduino). SPI devices communicate in full duplex mode which allow simultaneous data transmission in both directions using a master-slave architecture. SPI protocol can only support one master and multi-slaves through slave selection (SS), so we decided to put all thermocouple amplifiers on one PCB. We soldered the thermocouple amplifiers on a breadboard and connected all the chips in series. This means that we soldered all the corresponding pins together except the chip select pins (CS). The chip select pins are directly soldered on the different digital pins on the Arduino, because the SPI interface only can select one chip at a time.

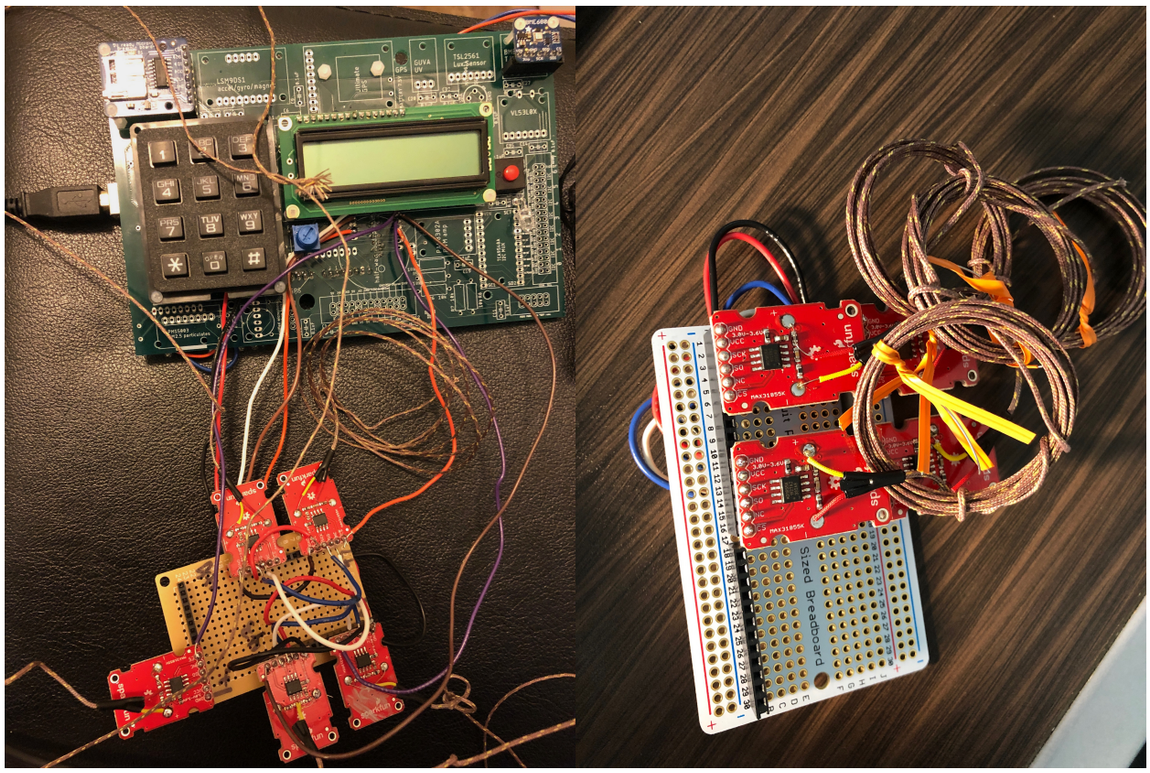

(a) Printed Circuit Board (b) Soldered Thermocouples

Figure 4: Our final printed circuit board and zoom in of attatched thermocouples.

1.1.5 Data Acquisition Software

Our data acquisition software (DAQ) was written entirely in Arduino and allows us to take measurements from all thermocouples at once. In the DAQ, each thermocouple is assigned to a different digital pin on the Arduino itself, and since the thermocouple breakout boards function by SPI, the DAQ can record data from each thermocouple at once. Since four thermocouples are attached to one single PCB, the data acquired from all four thermocouples, as well as the room temperature are saved into a micro-SD card in .txt format. Then, our Python code read and handle the data.

1.2 Technical Background

The physics in this project is relatively straightforward in its use and purpose. Each thermocouple records the temperature relative to their internal thermometer at a given point. This allows us to draw an analogy between our system and a simple two-dimensional rectangular lattice. For different planes in the oven, we divide the region up into cells of uniform area. In the center of each cell, we place a thermocouple acting as a lattice point and assign the temperature that the thermocouple reads to the entire region within that cell. This allows us to choose a length scale parameter Λ over which to average by. We construct the mean temperature field $T_\Lambda(x, y)$ by shifting a region of area Λ^2 centered at the point (x, y) and summing over the contributions from each cell weighted by the overlap in area between the region of interest and the cell. We can do this analytically and numerically by integrating over each cell and only allowing the overlap to contribute to in the integral via:

$$T_\Lambda(x,y) = \frac{1}{\Lambda^2} \sum_{i=\text{cells}} T_i \int_{\text{cell } i} dudv\ \theta(u-(\Lambda-x/2))\theta(u+(\Lambda+x/2))\theta(v-(\Lambda-y/2))\theta(v+(\Lambda+y/2)), \tag{1}$$

where T_i is the temperature assigned to cell i from the thermocouple inside of it, and $\theta(x)$

is the Heaviside step-function. Changing the length scale Λ can greatly change how close this constructed mean temperature field is to the real temperature profile inside the oven, and there will be a specific length scale where the mean-field is as close to the true profile as possible. In physics, problems involving heat flow often involve finding analytic solutions to the heat equation in equilibrium by:

$$\frac{\partial T}{\partial t} = \kappa \nabla^2 T \tag{2}$$

for some prescribed boundary conditions. Ideally, our mean temperature field $T_\Lambda(x, y)$ would solve, or at least approximately solve the heat equation with Dirichlet boundary conditions. The error between T_Λ and a relatively close solution to the heat equation will be determined both by the crude means of constructing the mean-temperature field, properties of the oven itself, as well as our experimental setup.

There are a few more interesting quantities we can gather from the mean-temperature field. For convection ovens, we expect much larger temperature differences between different regions in the oven when compared to non-convection ovens. Studying the gradient of the temperature profile, will in theory, allow us to distinguish whether an oven is convective or non-convective. For example, near where the air is circulated, the temperature gradient should be much steeper in a convection oven, then in the center of a standard oven.

1.3 A Solution to the Heat Equation

In this section we present a tentative solution to the heat equation with relevant boundary conditions. The heat equation is well-posed and in order to solve it, we must specify boundary conditions in space and an initial condition in time. The heat equation problem that we wish to solve is:

$$\frac{\partial}{\partial t} T(\mathbf{x}, t) = \kappa \nabla^2 T(\mathbf{x}, t), \ \forall (\mathbf{x}, t) \in \Omega \times [0, \infty), \tag{3}$$

where $\Omega = [0, L_x] \times [0, L_y] \times [0, L_z]$ is the domain of the oven where the heat equation is defined and κ is a constant that represents heat diffusion. The boundary and initial boundary conditions are:

$$\begin{cases} T(\mathbf{x}, 0) = T_r, \ \forall \mathbf{x} \in \Omega \\ \partial_x T(0, y, z, t) = \partial_x T(L_x, y, z, t) = 0, \ \forall t \geq 0 \\ \partial_y T(x, 0, z, t) = \partial_y T(x, L_y, z, t) = 0, \ \forall t \geq 0 \\ \partial_z T(x, y, L_z, t) = 0, \ \forall t \geq 0 \\ T(x, y, 0, t) = T_o, \ \forall t \geq 0 \end{cases}$$

where T_r is the constant room temperature and T_o is the oven temperature set before each trial. We assume the heat source is at the bottom of the oven, thus we only set the bottom of the oven to be T_o. To solve the problem, we assume (due to constant boundary conditions) the temperature inside the oven becomes independent of time in the steady state limit $t \to \infty$. Let $T_E(\mathbf{x})$ be the equilibrium temperature sufficiently large t. We should have:

$$\lim_{t \to \infty} T(\mathbf{x}, t) = T_E(\mathbf{x}), \ \forall \mathbf{x} \in \Omega. \tag{4}$$

From which it follows that:

$$\nabla^2 T_E = \kappa \frac{\partial}{\partial t} T_E = 0 \tag{5}$$

$$\begin{cases} \partial_x T_E(0, y, z) = \partial_x T_E(L_x, y, z) = 0 \\ \partial_y T_E(x, 0, z) = \partial_y T_E(x, L_y, z) = 0 \\ \partial_z T_E(x, y, L_z) = 0 \\ T_E(x, y, 0) = T_o \end{cases}$$

Therefore T_E is harmonic inside Ω and satisfies the above boundary conditions. We now state the uniqueness theorem which makes our calculation of T_E trivial.

Theorem 1 (Uniqueness Theorem) *For a given domain Ω and above boundary conditions, if T_E and T'_E are two harmonic functions that satisfy the given boundary conditions then $T_E = T'_E$.*

Clearly $T_E = T_o$, the constant function, satisfies both Laplace's equation and the boundary conditions. Therefore we must have:

$$T(\mathbf{x}) = T_o. \tag{6}$$

Now, consider function $u(\mathbf{x}, t) := T(\mathbf{x}, t) - T_E(\mathbf{x})$, where $u(\mathbf{x}, t)$ satisfies the homogeneous heat equation:

$$\frac{\partial}{\partial t} u(\mathbf{x}, t) = \nabla^2 u(\mathbf{x}, t) \tag{7}$$

$$\begin{cases} u(\mathbf{x}, 0) = T_r - T_E(\mathbf{x}) = T_r - T_o, \ \forall \vec{\mathbf{x}} \in \Omega \\ \partial_x y(0, y, z, t) = \partial_x u(L_x, y, z, t) = 0, \ \forall t \geq 0 \\ \partial_y u(x, 0, z, t) = \partial_y u(x, L_y, z, t) = 0, \ \forall t \geq 0 \\ \partial_z u(x, y, L_z, t) = 0, \ \forall t \geq 0 \\ u(x, y, 0, t) = 0, \ \forall t \geq 0 \end{cases}$$

Now it is possible to assume an eigenfunction expansion of $u(\mathbf{x}, t)$ inside Ω. The eigenvalue problem we are considering is the Dirichlet eigenvalue problem of the Laplacian operator:

$$\nabla^2 v = -\lambda v. \tag{8}$$

here $v \in C^2(\Omega)$ has no time dependence and satisfies our boundary conditions. The solutions for v that come from solving this eigenvalue problem are:

$$v_{n,m,\ell} = \cos \frac{n\pi x}{L_x} \cos \frac{m\pi y}{L_y} \sin \frac{\pi(\ell + \frac{1}{2})z}{L_z} \tag{9}$$

It can be shown that these functions are complete with respect to the L^2 norm, that is

$$\forall f \in C^2(\Omega) \bigcap L^2(\Omega), \ \exists \{A_{nm\ell} \in \mathbb{R}\}, \text{ s.t. } \lim_{N,M,L \to \infty} \int_\Omega \left| f - \sum_{\substack{n=N \\ m=M \\ \ell=L}}^{\infty} A_{nm\ell} v_{nm\ell} \right|^2 dx = 0. \tag{10}$$

Expanding the solution to the homogoneous heat equation, $u(\mathbf{x}, t)$ yields:

$$u(\mathbf{x}, t) = \sum_{n,m,\ell} a_{nm\ell}(t) v_{nm\ell} \tag{11}$$

Plugging $u(\mathbf{x}, t)$ back into the heat equation, we get a a set of first order differential equations for the coefficients $a_{nm\ell}(t)$'s, the initial condition of the heat equation gives the initial conditions for the coefficients:

$$\frac{\partial}{\partial t}a_{nm\ell}(t) = -\lambda_{nm\ell}a_{nm\ell}(t),\ a_{nm\ell}(0) = \frac{\int_\Omega (T_r - T_E(\mathbf{x}))v_{nm\ell}(\mathbf{x})dx}{\int_\Omega (v_{nm\ell}(\mathbf{x}))^2 dx} \tag{12}$$

The solutions are clearly

$$a_{nm\ell}(t) = a_{nm\ell}(0)e^{-\lambda_{nm\ell}t} \tag{13}$$

Substituting the coefficients back in yields a full solution. Plugging in $T_E(\mathbf{x}) = T_o$ and the solution of $v_{nm\ell}$ into equation (12) gives $a_{nm\ell} = 16\delta_{n0}\delta_{m0}/(2\ell+1)\pi$. So the final solution to the heat equation with our boundary conditions is:

$$T(\vec{\mathbf{x}}, t) = T_o + \frac{16(T_r - T_o)}{\pi}\sum_{\ell\in\mathbb{N}}\frac{1}{(2\ell+1)}\sin\left(\frac{\pi(\ell+\frac{1}{2})z}{L_z}\right)e^{-\pi(\ell+\frac{1}{2})\kappa t/L_z}. \tag{14}$$

Methodology and Experimental Procedure

(a) Example shot of layout of thermocouples on lower rack at front of the oven.

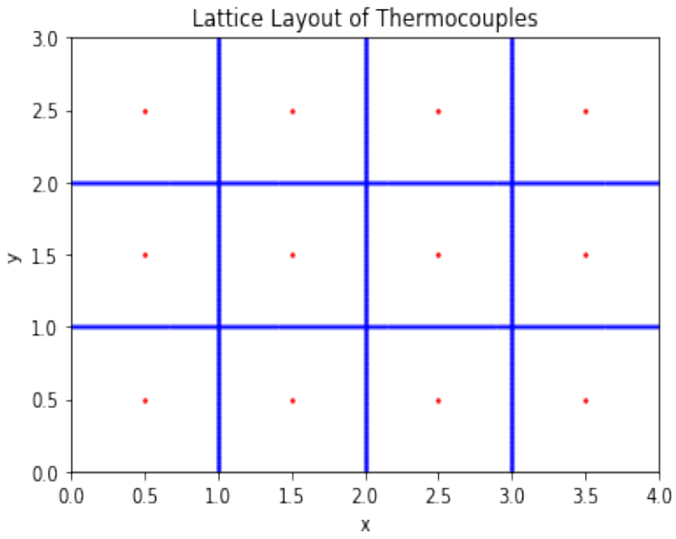

(b) Idealized lattice layout of thermocouples. $y = 0$ represents the back of the oven, while $y = 3$ represents the front of the oven where the oven door is. x is in units of $L_x/4$ while y is in units of $L_y/3$, just for clarity.

Figure 5: Lattice layout during experiment of taking down on lower rack near the front of the oven and idealized theory layout of thermocouples.

As discussed previously, for the experimental procedure, we laid out each thermocouple soldered to our printed circuit board in the shape of a rectangular lattice. As we have only four thermocouples soldered to a single circuit board, we had to take three different measurements for a single plane in the oven. The oven used has two racks, which were chosen to be the two planes studied in this paper. Unfortunately, our thermocouples are about 1m long, so not all four can reach the back of the oven. For these measurements, we could only take data with two thermocouples.

After the thermocouples were installed inside the oven, the oven is turned on with the "Bake" mode with the temperature set to 180. The oven door is then shut and the oven enters the "pre-heat" procedure. This is when the oven is heated to the preset temperature. Once heated to the preset temperature, the oven enters the baking period. After the oven is turned on for 30 minutes, the oven is turned off and enters the cooling period. After cooling for 30 minutes, we stop taking data. The oven we used for our experiments had a width $L_x = .61$cm, a length of $L_y = 41.91$cm and a height of $L_z = .61$cm.

The data for freezer and fridge is taken using the same methodology. We place the thermocouples in an evenly distributed line in the freezer and fridge. And again, just as the case of the oven we do this for the front, the middle and the back of the fridge. The data was taken for the whole night but we will only show a fraction of them.

Figure 6: Fridge and thermocouples.

Figure 7: Freezer and thermocouples.

Results and Discussion

1.4 Calibration

We first calibrated our thermocouple temperatures, and adjusted our later measurements according to this calibration. Figure 8(a) and 8(b) are calibration plots and their respective zoomed-in versions for thermocouple set 1, and figures 8(c) and 8(d) are for thermocouple set 2. We put all four thermocouples as close together as possible and heat the oven up to 180° C. Since all thermocouples are very close to one another, if they were perfectly calibrated the temperatures should be exactly the same. However, because this is not the

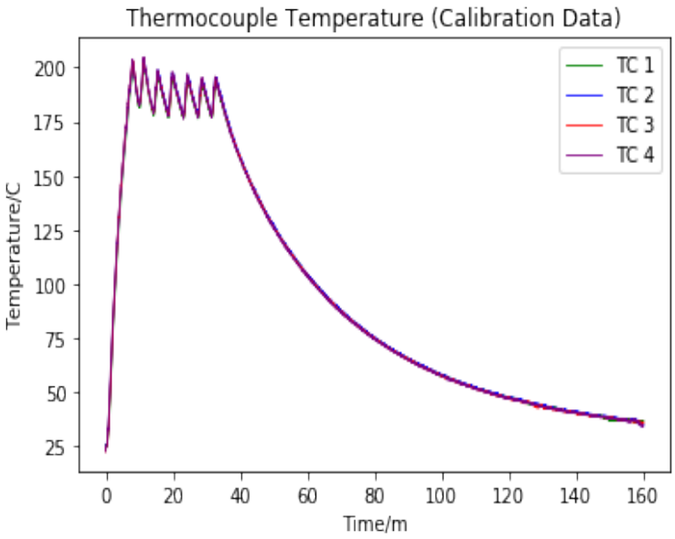

(a) Calibration data for first set of thermocouples.

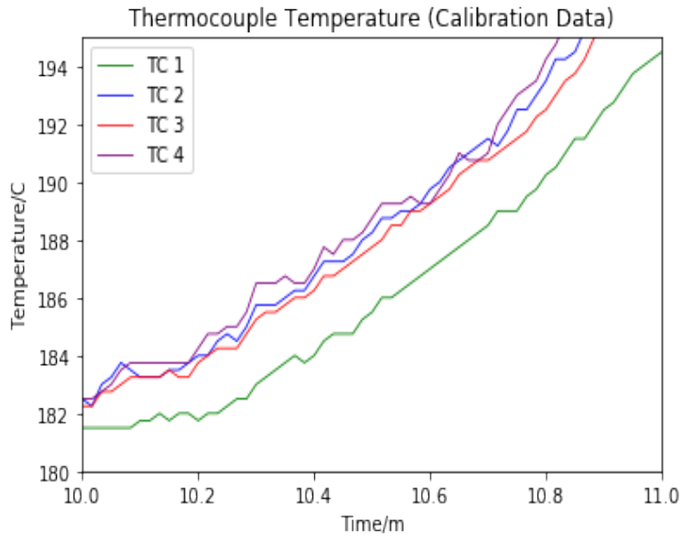

(b) Zoomed in plot of $8a$ between $t = 600$s and $t = 660$s.

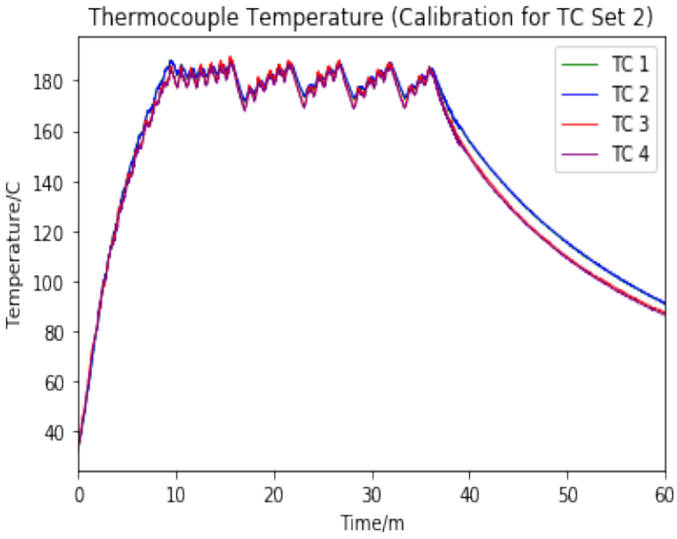

(c) Calibration data for second set of thermocouples.

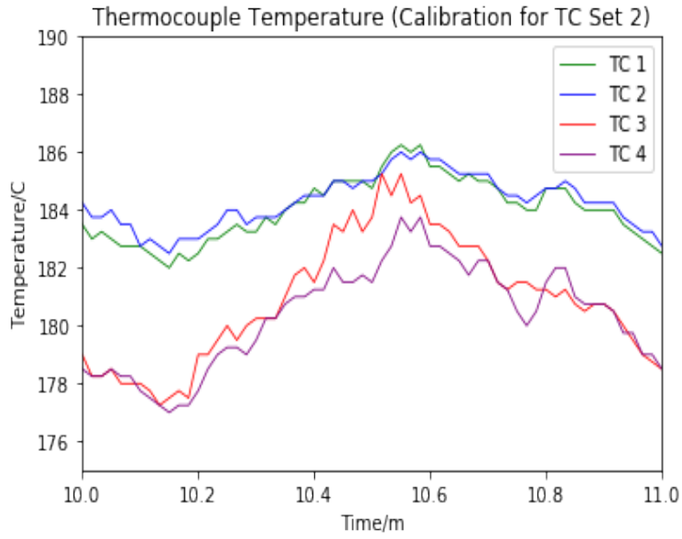

(d) Zoomed in plot of $8c$ between $t = 600$s and $t = 660$s.

Figure 8: Plots of calibration data for both sets of thermocouples used.

case we have to choose which thermocouples we consider "good" and shift the temperatures according to that choice.

For thermocouple set 1, we took the mean temperature measured by thermocouples $2, 3, 4$ as the actual temperature and shifted the first one temperature up by $\approx 2°$ C to match the actual temperature. For thermocouple set 2, we took the mean temperature measured by thermocouples 1 and 2 to be the actual temperature, and shifted the temperatured of thermocouples 3 and 4 up by $\approx 6°$ C to match them. We used thermocouple set 1 to take the data for the oven and freezer, and thermocouple set 2 to take data for the fridge. The calibration data for the second set of thermocouples as seen in figures $8c$ and $8d$ were taken using a different electric oven. This explains why the behavior once the thermocouples have reached equilibrium with the oven is different between the plots of different thermocouple sets.

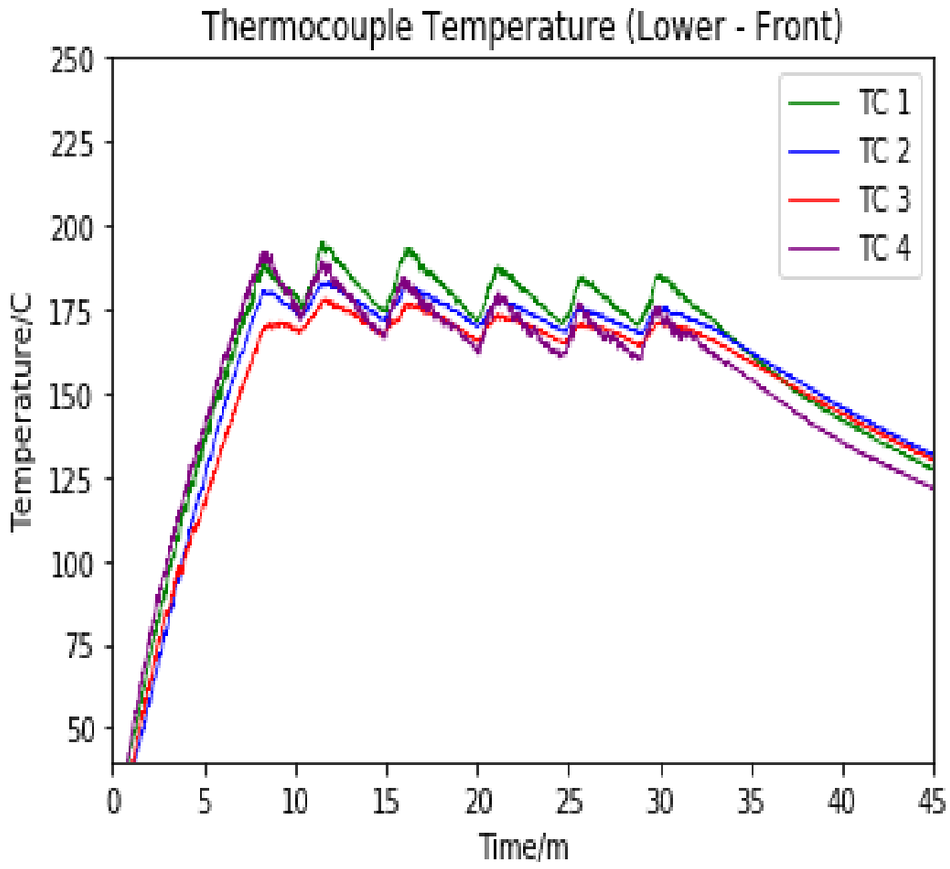

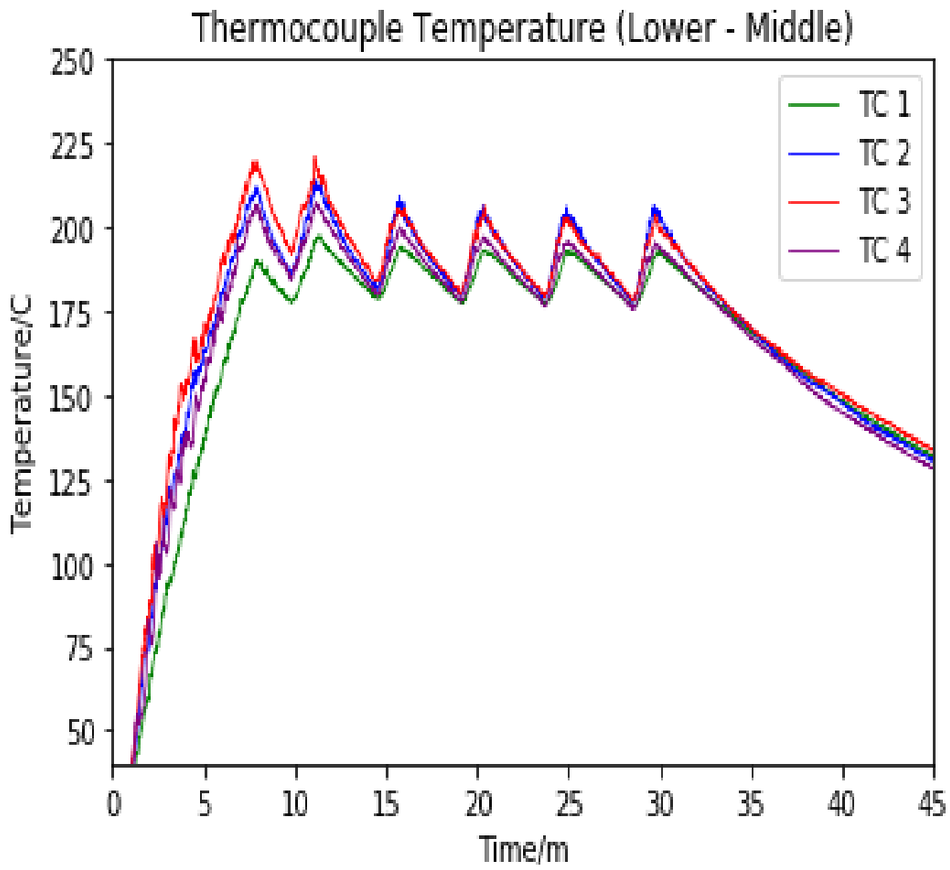

(a) Thermocouple temperatures for the front of the lower shelf.
(b) Thermocouple temperatures for the middle of the lower shelf.

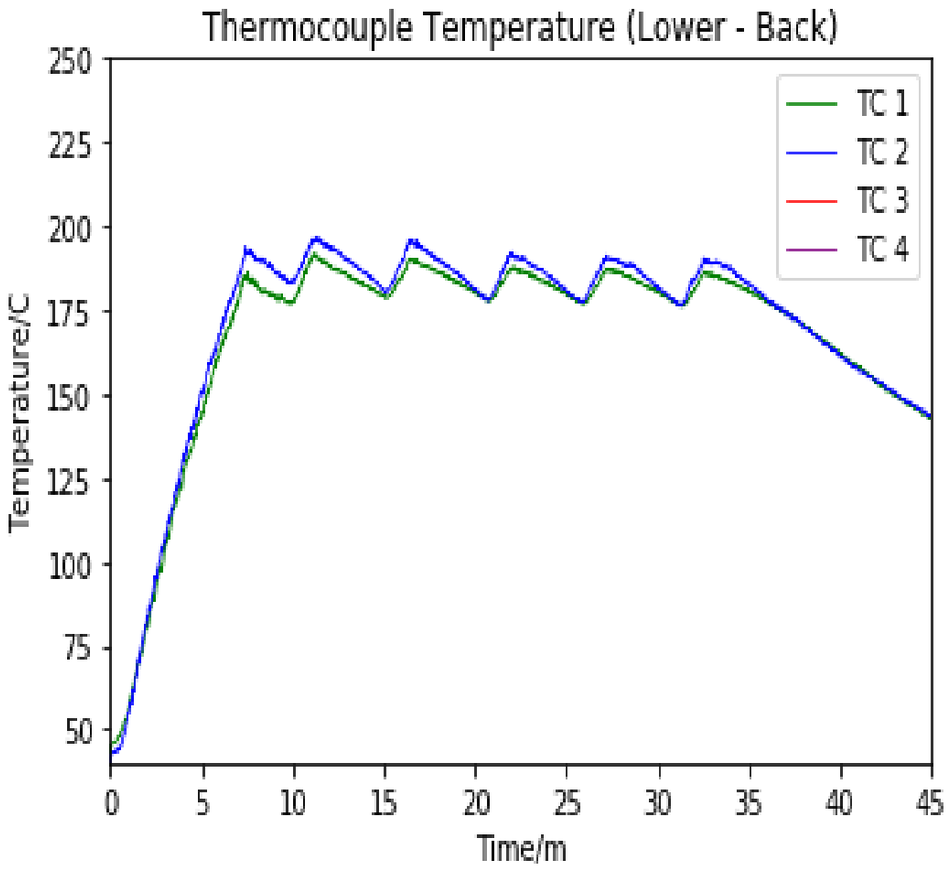

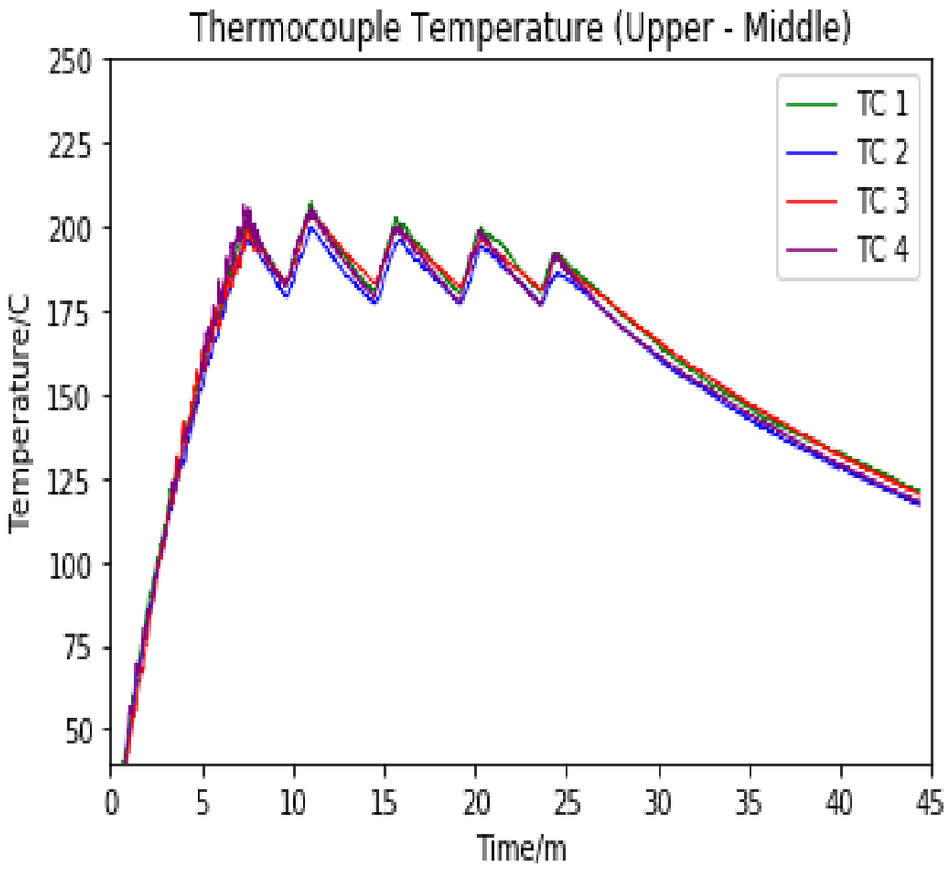

(c) Thermocouple temperatures for the back of the lower shelf. There are only two thermocouples shown here, as only these two could reach into the back.

(d) Thermocouple temperatures for the middle of the upper shelf.

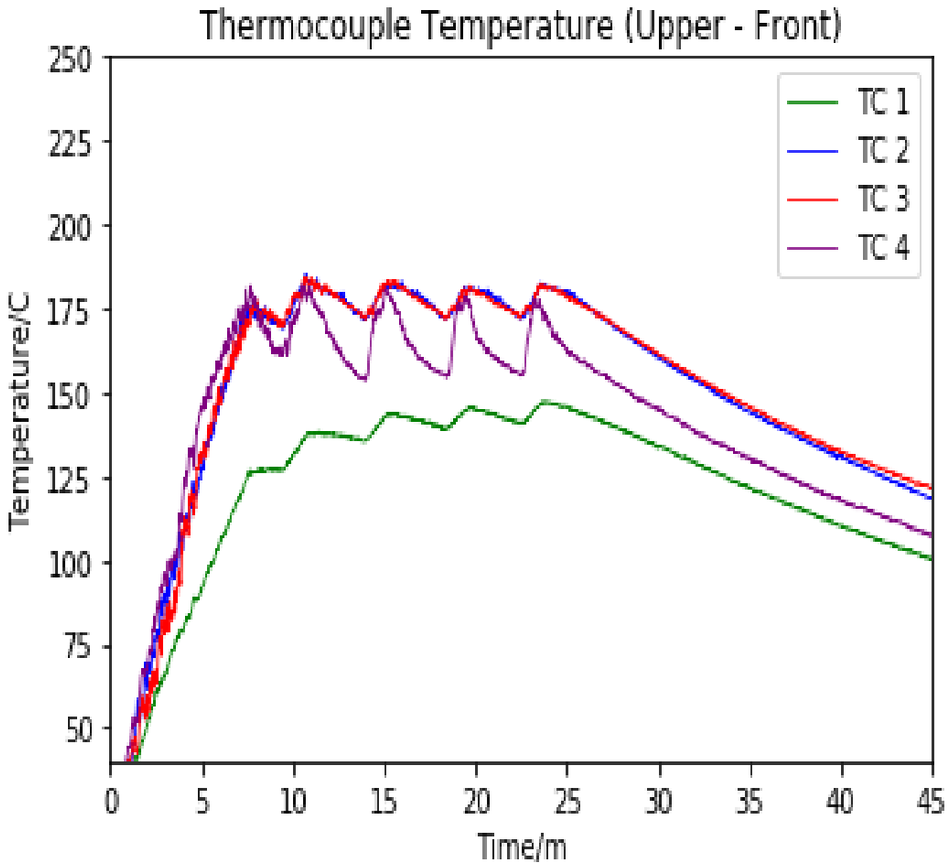

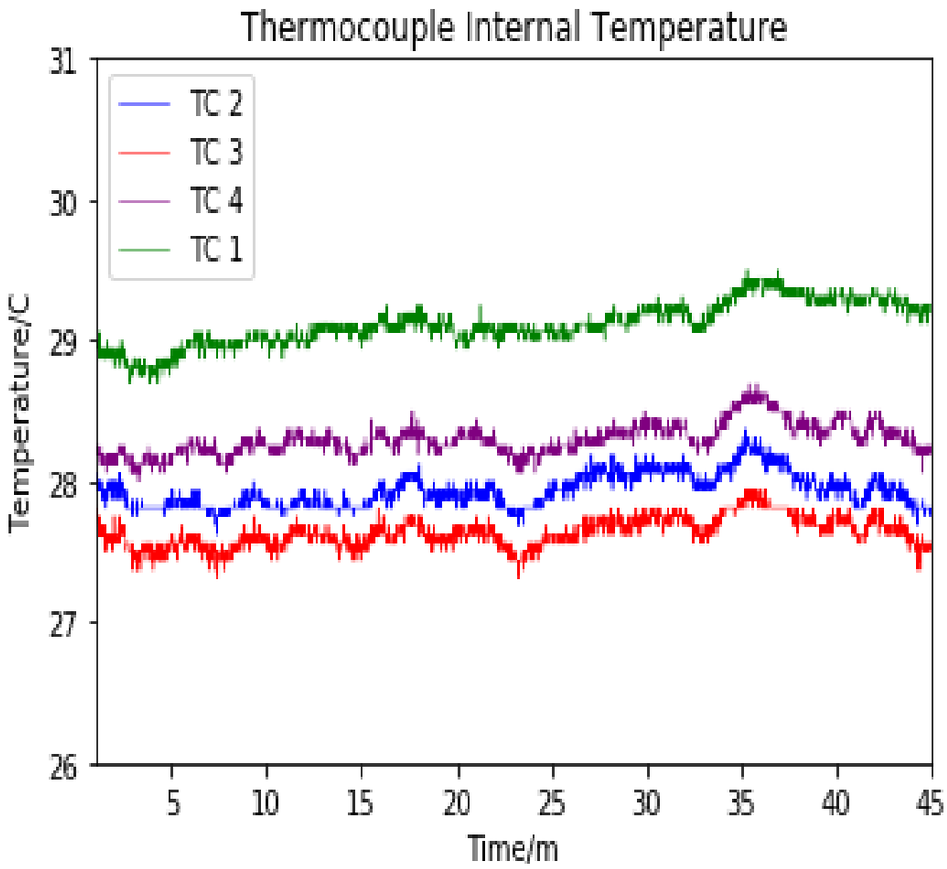

(e) Thermocouple temperatures for the front of the upper shelf. Strange behavior of TC 1 discussed below.
(f) Internal thermocouple temperature.

Figure 9: Thermocouple temperature and internal temperature data versus time.

1.5 Qualitative Analysis

1.5.1 Oven

The most defining common feature of these curves is the saw-tooth shape that they share. We suspect this is due to natural cooling of the oven when the oven is heating to its set temperature. In these experiments, the temperature of the oven is set at 180° Celsius. Therefore, to keep the temperature in the oven at the desired setting, the oven turns the heat off once the temperature around the sensors inside the oven is too high. Once the heat is turned off is activated, the temperature in the oven starts to drop. When the temperature around the sensors is too low, the oven starts to heat up again to offset the induced undershooting of the temperature from the natural cooling of the oven. This explains the sudden drop in temperature inside the oven. In figure 9*e*, there is one thermocouple (TC 1) that has a much lower temperature than the rest. These measurements were taken with the same set of thermocouples, so we have no way to explain this behavior outside of it being an issue with the oven itself.

Another interesting piece of information is that the maximum temperature reached by the thermocouples in different positions is not the same. Take figure 9*b* for instance, the maximum temperature reached by the red curve is $\approx 225°$ C, while the green curve only $\approx 200°$ C. This occurs when the temperature in the oven is set to 180° C. This is likely is because the position of the temperature sensors inside the oven is close to or on the walls of the oven. Hence, due to the unevenness of the temperature distribution inside the oven, we conducted the experiment with, by the time the temperature near the walls reaches the desired setting, the temperature in the middle has already greatly increased. As shown in the picture, this temperature difference between the center of the plane of the oven and the sides can be quite large, even up to $\sim 50°$ C.

1.5.2 Fridge and Freezer

The data for the freezer shows similar saw-tooth shape as the oven data. The data shows that after the door is shut, the freezer starts to cool down to approximately $-12.5°$ C. Then the compressor stopped working and restarted when the temperature rises to $-9°$ C. This pattern repeats until the thermocouples are turned off. In addition, we observed a sharp peak in each cycle but we expect the temperature transition will be more smooth.

We can see that the plots for the fridge share similar characteristics to those of the freezer. Just like the freezer, the fridge has cycles where the fridge cools to a desired temperature of around 8° C, and then stops. This causes the temperature to rise a couple of degrees after which the fridge starts cooling again. However the temperature of thermocouple four which is on the left side of the fridge is significantly lower than the other three in the first 30 minutes. The reason might be that there are some heat-absorbing items, such as hot meal, on the right side of the refrigerator, so we don't observe very sharp peaks when the cooling begins again.

1.6 Quantitative Analysis

We have the plots for the coarse-grained mean-temperature field $T_\Lambda(x, y)$ for $\Lambda = L_x/30$, where L_x is the dimension of the oven in the x-direction. Just from the heat maps alone, we notice a lot of interesting tidbits on how ovens operate during the cooling and heating

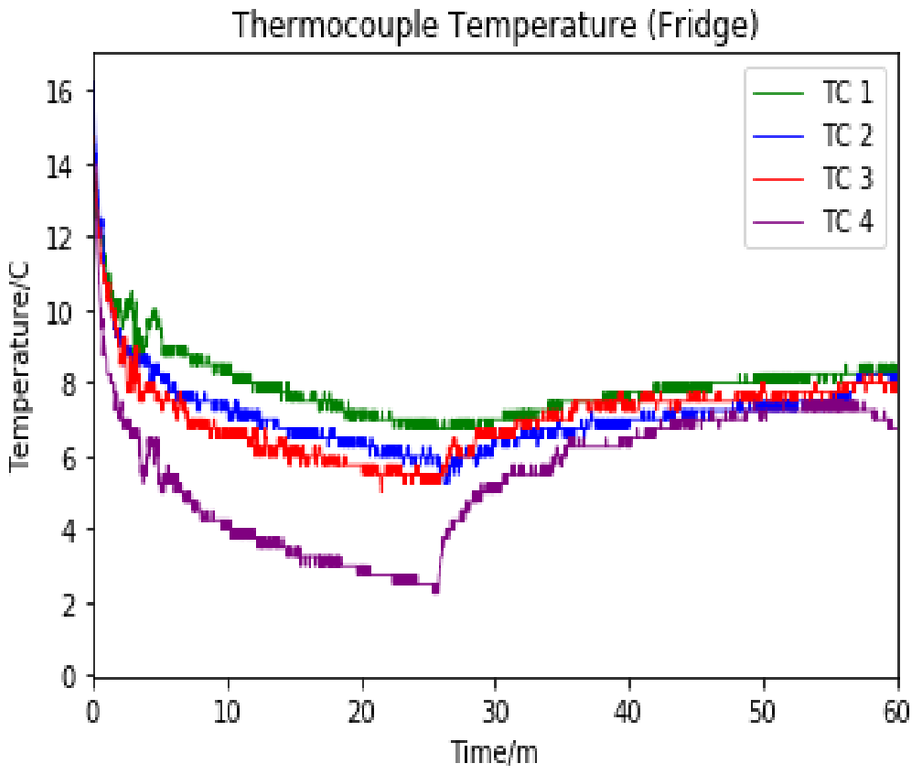

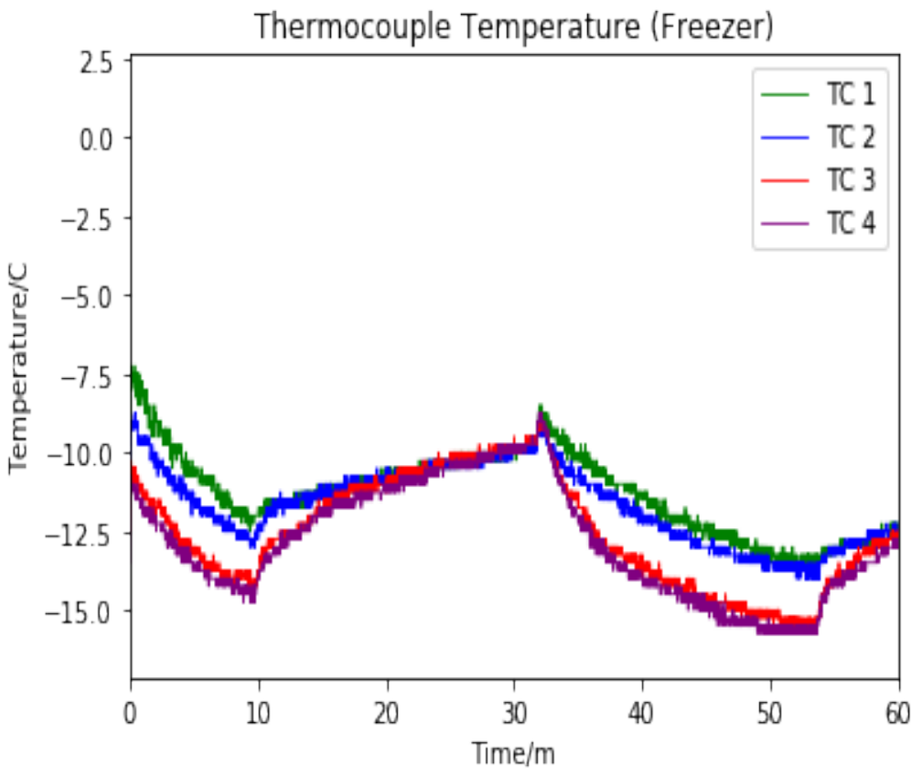

(a) Temperature profile for the fridge
(b) Temperature profile of the freezer

Figure 10: Thermocouple fridge and freezer plots.

processes. For $t = 300$s in figure 11a, we chose the time such that the oven is in the process of heating up, we see that the oven is much cooler near the circumference, especially the front. This tells us that the heat source of the oven is in the middle bottom of the oven. At $t = 1200$s in figure 11b, the oven reaches the equilibrium. We see the temperature is still relatively hot in the middle compare to its surroundings. We postulate from this that the oven is poorly insulated, thus while the oven is trying to reaming in equilibrium, there is still a large amount of heat leaking out on the edges. Lastly, figures 11c and 11d are for $t = 2100$s

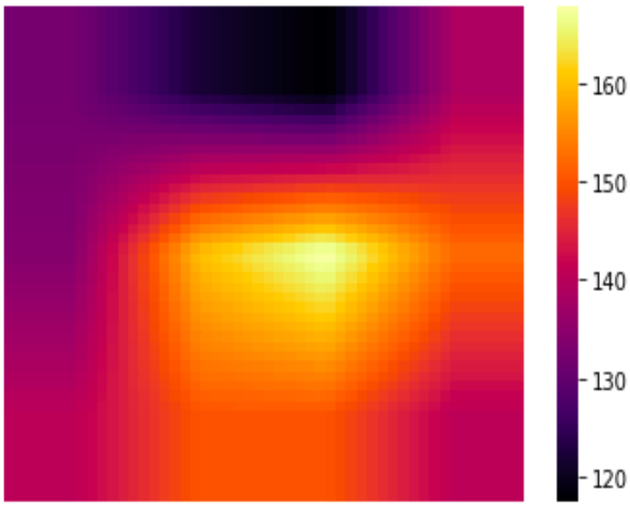

(a) $T_\Lambda(x, y)$, $t = 300$s

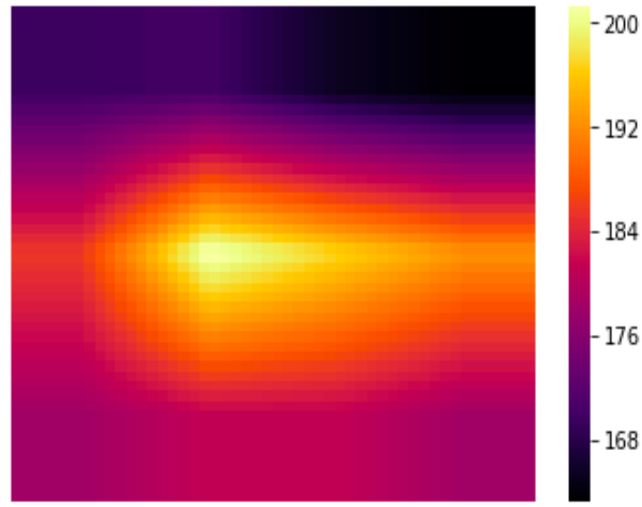

(b) $T_\Lambda(x, y)$, $t = 1200$s

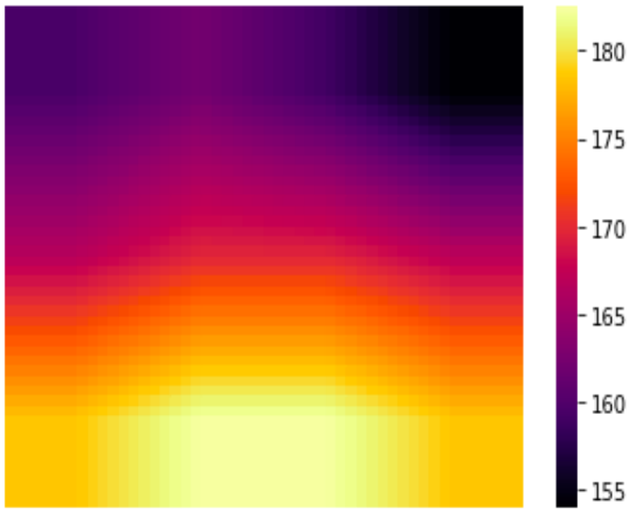

(c) $T_\Lambda(x, y)$, $t = 2100$s

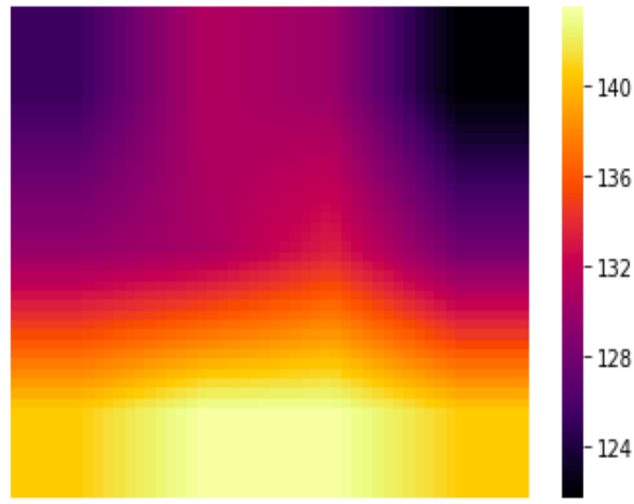

(d) $T_\Lambda(x, y)$, $t = 2700$s

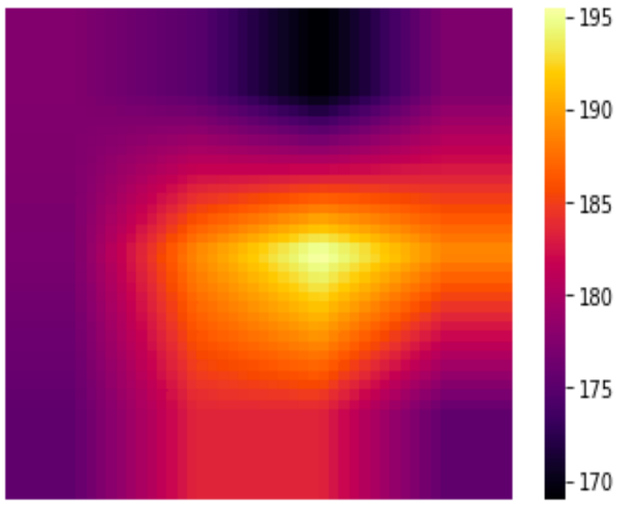

(e) Mean-field temperature in a peak.

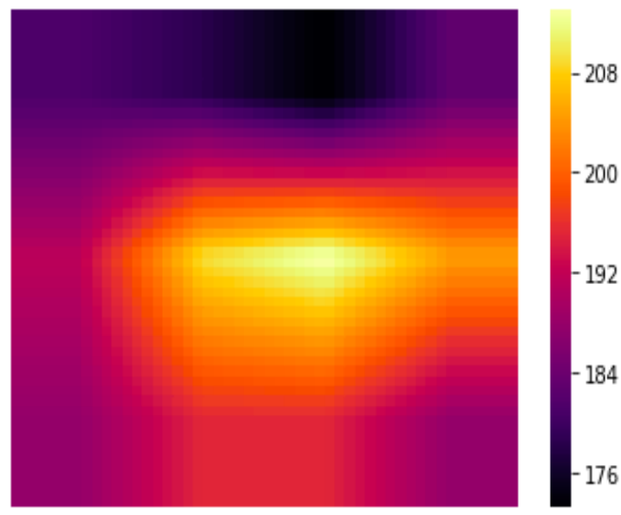

(f) Mean-field temperature in a trough.

Figure 11: Plots of the mean temperature field for different times for the lower rack. The bottom of the plots represents the back of the oven, and the top represents the front where the oven door is located.

and $t = 2700$s respectively. Figure 11c is when the oven is starting to cool down, and 11d is when the oven has been cooled down for a while. We see the temperature of the oven is

the hottest during the process of heating up and in equilibrium; this makes sense because the heating source of the oven is in the middle of the bottom rack,therefore the middle heats up first before other parts do. When the oven starts to cool down, we see the first region that starts to cool down is the front of the oven, which matches our intuition of heat leaking out through the front. Figures 11e and 11f are plots when the thermocouples have reached equilibrium with the oven, where all the thermocouples are in the same peak or trough in the temperature plots in figure 9. This is because there are some differences between each experiment, so to get accurate mean field plots we should correct for this. In general, The mean-temperature fields also tend to be very smooth in space, as there are no sharp drop-offs in their values which suggests this choice of scale parameter Λ is a good choice. We expect then that these profiles will approximately solve the heat equation.

We can learn a lot about comparing the coarse-grained temperature field T_Λ to our solution of the heat equation $T(\mathbf{x}, t)$. Firstly, we notice that for a plane of fixed z height in the oven, $T(\mathbf{x}, t)$ is constant in space. The solution to the heat equation has no dependence in the x- and y-directions, where we can see that this is not the case for the mean-field temperature. We also notice that the solution to the heat equation decays in time as $T(\mathbf{x}, t) \sim e^{-\kappa t/L_z}$. This is the complete opposite of the data we recorded when the oven is heating which grows exponentially in time. This is most likely due to some incorrect choice in boundary conditions.

Conclusion

Lastly, we see that simple data measurements taken with our thermocouples laid out in different positions can tell us a great deal about the oven. Even if our experimental configuration was quite simple and we did not have many thermocouples to work with. The first thing of significance we note is that the temperature distribution inside the oven can be very uneven. One can see this by looking at the graphs of thermocouple temperature versus time, or through the heat map, which display the temperature distribution more vividly. For instance, the temperature difference between different regions inside the oven can be over 30 degrees for a given time.

Secondly, we note there is a certain mechanism to prevent the oven from overshooting or undershooting. And that is the same for our fridge and freezer. One can see this through the saw-tooth shape in our plots above. Since our oven has no fans, we suspect this mechanism is simply natural cooling by which we mean turning on and off the heating system. However, even with this mechanism, the temperature in the middle still goes up to 225° C, even though the oven is set at 180° C. Hence, we conclude the temperature sensor of the oven is on the walls where the temperature appears to be lower.

Finally, we note the heat equation solution fits poorly with our data of the oven, which is expected. To see this, note the solution is constant for fixed height, but this is clearly not the case of the measurement. On the other hand, this implies the oven is not well insulated. Because the boundary condition we solved for the heat equation assumes the oven is perfectly insulated, and the fitting precisely implies the contrary.

References

[1] *BOSCH (July, 2017). BME680 Low power gas, pressure, temperature humidity sensor.PDF file, pp. 10-13.*

[2] *F. Leens, "An introduction to I2C and SPI protocols," in IEEE Instrumentation Measurement Magazine, vol. 12, no. 1, pp. 8-13, February 2009.*

[3] *Maxim Innovation Delivered (February 2012). "MAX31855 Cold-Junction Compensated Thermocouple-to-Digital Converter. PDF file, pp. 7-8.*

[4] *Olumodeji, O. A., Gottardi, M. (2017). Arduino-controlled HP memristor emulator for memristor circuit applications. Integration: The VLSI Journal, 58, 438–445.*

[5] *McOwen, R. (2002). Partial Differential Equations,: Methods and Applications, Chapter 5.*

[6] *https://www.adafruit.com/product/269*

[7] *https://www.adafruit.com/product/3660*